ORGANOMETALLICS

Article

pubs.acs.org/Organometallics

β-H Abstraction/1,3-CH Bond Addition as a Mechanism for the Activation of CH Bonds at Early Transition Metal Centers

Yimu Hu,[†,‡] Nuria Romero,[†,‡] Chiara Dinoi,[†,‡] Laure Vendier,[†,‡] Sonia Mallet-Ladeira,[§] John E. McGrady,[∥] Abel Locati,[⊥] Feliu Maseras,[⊥,#] and Michel Etienne*[,†,‡]

[†]CNRS, LCC (Laboratoire de Chimie de Coordination), 205, route de Narbonne, BP 44099, F-31077 Toulouse Cedex 4, France

[‡]Université de Toulouse, UPS, INPT, LCC, F-31077 Toulouse Cedex 4, France

[§]Institut de Chimie de Toulouse (FR 2599), Université Paul Sabatier, 118, route de Narbonne, F-31062 Toulouse Cedex 9, France

[∥]Department of Chemistry, Inorganic Chemistry Laboratory, University of Oxford, South Parks Road, Oxford OX1 3QR, United Kingdom

[⊥]Institute of Chemical Research of Catalonia (ICIQ), Av. Paisos Catalans, 16, 43007 Tarragona, Spain

[#]Departament de Química, Universitat Autònoma de Barcelona, 08193 Bellaterra, Spain

Supporting Information

ABSTRACT: This article describes the generalization of an overlooked mechanism for CH bond activation at early transition metal centers, namely 1,3-CH bond addition at an η^2-alkene intermediate. The X-ray-characterized $[Cp_2Zr(c\text{-}C_3H_5)_2]$ eliminates cyclopropane by a β-H abstraction reaction to generate the transient η^2-cyclopropene $[Cp_2Zr(\eta^2\text{-}c\text{-}C_3H_4)]$ intermediate **A**. **A** rapidly cleaves the CH bond of furan and thiophene to give the furyl and thienyl complexes $[Cp_2Zr(c\text{-}C_3H_5)(2\text{-}C_4H_3X)]$ (X = O, S), respectively. Benzene is less cleanly activated. Mechanistic investigations including kinetic studies, isotope labeling, and DFT computation of the reaction profile all confirm that rapid stereospecific 1,3-CH bond addition across the Zr(η^2-alkene) bond of **A** follows the rate-determining β-H abstraction reaction. DFT computations also suggest that an α-CC agostic rotamer of $[Cp_2Zr(c\text{-}C_3H_5)_2]$ assists the β-H abstraction of cyclopropane. The nature of the α-CC agostic interaction is discussed in the light of an NBO analysis.

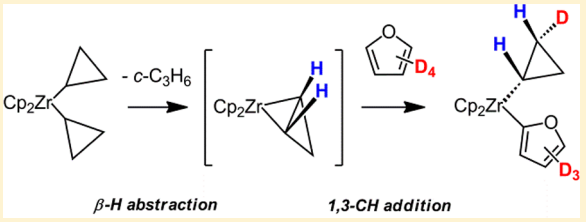

INTRODUCTION

The general problem of activating strong and inert CH bonds of hydrocarbons by soluble catalysts continues to fascinate chemists, although it is becoming increasingly more practical and reaches the genuine catalytic functionalization stage on many occasions.[1−3] One remaining pressing issue is the selectivity for different types of CH bonds;[4−6] addressing this issue requires the investigation of different mechanisms by which a transition metal complex cleaves a given CH bond. Oxidative addition and electrophilic activation,[7−12] with some recent variations (AMLA,[13] CMD,[14] σ-CAM,[15] 1,2-addition[16]), characterize the reactivity of late transition metal complexes. High-valent early transition metal complexes tend to activate CH bonds by two main pathways (Scheme 1): σ-bond metathesis[17−20] in L_nMR and 1,2-CH bond addition across MX multiple bonds of transient unsaturated L_nMX such as imido M═NR,[21−28] alkylidene M═CRR′,[29−33] or alkylidyne Ti≡CR complexes.[34−36]

Often these intermediates are generated by α-H abstraction from alkyl amido, dialkyl, or alkyl alkylidene complexes—the microscopic reverse of 1,2-CH bond cleavage. In a seminal paper,[37] Erker demonstrated that diaryl zirconocenes would equilibrate via the transient intermediate $[Cp_2Zr(\eta^2\text{-aryne})]$ by reversible β-H abstraction/1,3-CH bond activation of an arene

Scheme 1. CH Bond Activation Schemes at Early Transition Metal Centers

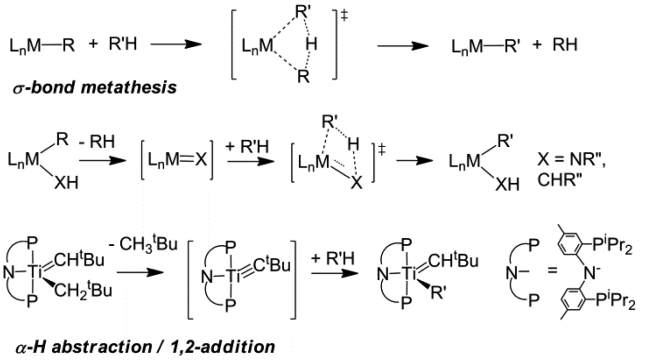

(Scheme 2). This is now a well-documented reaction for η^2-benzyne complexes of several early transition metals.[32−34,38] Unsaturated terminal alkyne complexes have also activated CH bonds of hydrocarbons via this mechanism.[39,40] As sketched in Scheme 1, transition states for either 1,2- or 1,3-CH bond

Received: October 20, 2014

   dx.doi.org/10.1021/om501056b | Organometallics XXXX, XXX, XXX−XXX

Scheme 2. Examples of β-H Abstraction/1,3-CH Bond Addition

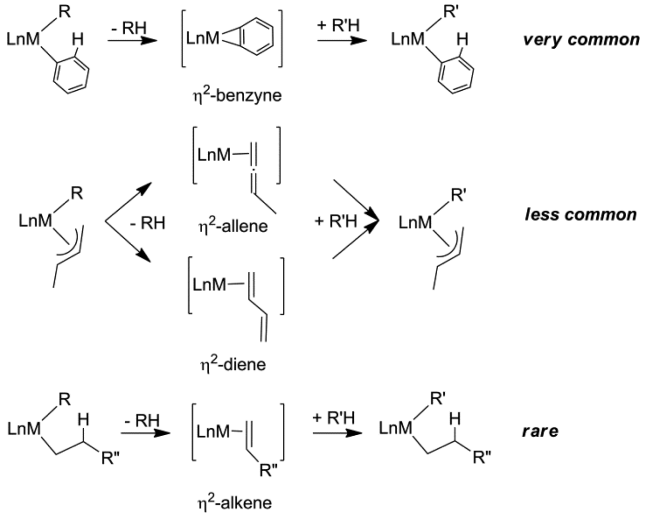

cleavage have a distinctive σ-bond metathesis type of geometry, where a proton is formally transferred between two negatively charged carbons.[41]

Other cases where this reaction becomes competitive in the presence of α-hydrogens are rare: examples include CH activation on η^2-allene and η^2-diene intermediates generated from alkyl allyl complexes of the type [Cp*M(NO)(R)(η^3-CH_2CHCHR)] (M = Mo, W).[42−45] *Inter*molecular 1,3-CH addition across an $L_nM(\eta^2$-alkene) to yield an alkyl hydrocarbyl complex remains uncommon[46] and occurs only with the more reactive CH bonds, such as those of terminal alkynes.[47,48] In other words, β-H abstraction is rarely reversible in this case.[49,50] Isomerization of coordinated alkenes to alkylidenes has been realized in [(silox)M(η^2-alkene)] (silox = *t*-Bu_3SiO, M = Nb, Ta) complexes, where reversible *intra*molecular α-, β-, or δ-H abstractions were all involved in the rearrangement.[51] Unsaturated early transition metal $L_nM(\eta^2$-alkene) may undergo alkene substitution or alkene coupling reactions.[52] Also alkyl complexes bearing β-hydrogens tend to decompose by β-H elimination to give alkene hydride complexes.

We reported on a very mild activation of benzene and alkyl aromatic CH bonds by the methyl cyclopropyl niobium complex [Tp^{Me_2}NbMe(*c*-C_3H_5)(MeCCMe)].[53,54] β-H abstraction of methane yields a transient unsaturated η^2-cyclopropene intermediate, [Tp^{Me_2}Nb(η^2-*c*-C_3H_4)(MeCCMe)], that is stable and reactive enough to undergo 1,3-CH bond activation of RH across the Nb−cyclopropene bond to yield the products [Tp^{Me_2}NbR(*c*-C_3H_5)(MeCCMe)]. Although [Tp^{Me_2}NbMe(*c*-C_3H_5)(MeCCMe)] shows an α-CC agostic cyclopropyl group,[55] there was no evidence that this unusual property[56] was at the origin of the rate-determining β-H abstraction reaction. Given the ease with which this reaction occurred, it was clearly of interest to see whether other early transition metal complexes would be capable of similarly mild CH bond activation reactions. Indeed, we report herein that (i) such simple complexes as zirconocene cyclopropyl complexes undergo β-H abstraction to yield η^2-cyclopropene intermediates as identified previously,[57] (ii) these unsaturated η^2-cyclopropene intermediates activate a CH bond of benzene or more reactive heteroaromatics by a 1,3-addition pathway for which a full mechanistic investigation is provided, and (iii) computational studies suggest that an α-CC agostic interaction assists the β-H abstraction reaction.

RESULTS AND DISCUSSION

Synthetic Aspects. The dicyclopropyl zirconocene Cp_2Zr-(*c*-$C_3H_5)_2$ (**1**) was synthesized from Cp_2ZrCl_2 and cyclopropyllithium according to a previously reported procedure.[58] Further characterization of **1** was needed for the purpose of the mechanistic studies described below. A ^{1}H NMR ROESY experiment in toluene-d_8 at 233 K established that the two equivalent C*H*α protons at δ −0.18 that appear as a triplet of triplets ($J_{H\alpha H\beta}$ = 10.0 Hz; $J_{H\alpha H\beta'}$ = 7.9 Hz) are on the same enantioface as the C*H*β (δ 0.78, dd, J = 10.0, 1.4 Hz), opposite to C*H*β' (δ 0.42, dd, J = 7.9, 1.4 Hz) (Scheme 3). The

Scheme 3. Stereochemistry in Cp_2Zr(*c*-$C_3H_5)_2$ (1) and Its Reactions with Aromatic Hydrocarbons

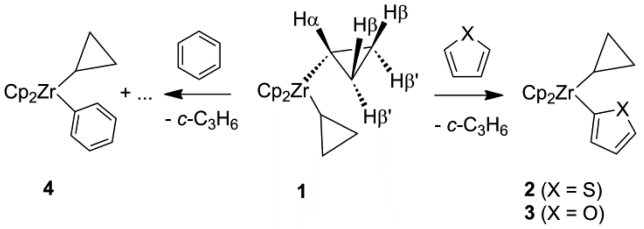

magnitudes of the J_{HH} values are consistent with the assignments. In the ^{13}C NMR, equivalent Cβ appear as a triplet at δ 10.2 ($^1J_{CH}$ = 158 Hz), whereas a doublet centered at δ 33.9 ($^1J_{CH}$ = 133 Hz) characterizes Cα. There is no evidence for either CH or CC agostic interactions.[54,59,60] An X-ray crystal structure has been obtained for **1** (see below).

The reactivity of **1** with aromatic hydrocarbons is summarized in Scheme 3. Complex **1** reacted readily (333 K, 24 h, either in a Teflon-valve-sealed NMR tube in cyclohexane-d_{12} or in cyclohexane solution in Schlenk tubes) with an excess of thiophene or furan to give the CH-activated cyclopropyl(2-thienyl)zirconocene [Cp_2Zr(*c*-C_3H_5)(2-C_4H_3S)] (**2**) and cyclopropyl(2-furyl)zirconocene [Cp_2Zr(*c*-C_3H_5)(2-C_4H_3O)] (**3**), along with cyclopropane and some unidentified decomposition products. No signals attributable to disubstituted or rearranged complexes were observed under these conditions.[61] **2** and **3** could be isolated in ca. 65% yield as yellow air- and moisture-sensitive solids. Reaction of **1** with the significantly less reactive benzene yielded what appears to be the phenyl cyclopropyl zirconocene [Cp_2ZrPh(*c*-C_3H_5)] (**4**), but it generated several unidentified byproducts (^{1}H NMR, see Supporting Information (SI)). Although the initial NMR spectra for **1** and [Cp_2ZrMe(*c*-C_3H_5)] were obtained from C_6D_6, the reaction with benzene was never mentioned.[57,58] The related cyclobutyl complex [Cp_2ZrMe(*c*-C_4H_7)] does generate the η^2-cyclobutene [Cp_2Zr-(η^2-*c*-C_4H_6)] intermediate readily, but no reaction with C_6D_6 was reported.[62]

Evidence for selective CH bond activation α to the heteroatom comes from the ^{1}H and ^{13}C NMR of **2** and **3**. For **2**, the 4-H proton of the thienyl group couples with both 3-H and 5-H and appears at δ 6.91 as a doublet of doublets (J_{H3H4} = 3.2; J_{H4H5} = 4.4 Hz, respectively). In the ^{13}C NMR spectrum of **2**, the zirconium-bound carbon ZrCS of the thienyl group appears at δ 176.7 and shows no direct coupling to hydrogen (J_{CH} = 15, 8 Hz). The 3-C (δ 127.1, ddd, J_{CH} = 163.2, 7.7, 5.4 Hz), 4-C (δ 130.8, dt, J_{CH} = 182.1, 8.8 Hz), and 5-C (δ 137.2,

dx.doi.org/10.1021/om501056b | *Organometallics* XXXX, XXX, XXX−XXX

ddd, J_{CH} = 162.4, 10.7, 5.9 Hz) give characteristic signals. ^{1}H and ^{13}C NMR signals identifying the cyclopropyl group are also observed (see SI). Similar ^{1}H and ^{13}C NMR spectra have also been observed for **3**. J_{HH} and a ^{1}H NMR ROESY experiment in C_6D_6 differentiated *Hβ* (*δ* −0.03, dd, *J* = 9.6, 2.2 Hz) from *Hβ′* (*δ* −0.45, dd, *J* = 7.9, 2.2 Hz) (SI, Figure S3). H*α* appeared as a multiplet at *δ* −0.17. Selective activation of the CH bond *α* to the heteroatom in furan and thiophene originates from its higher bond dissociation energy and lower pK_a, yielding a stronger ZrC bond in the product. As noted in the niobium case,[54] pyridine behaves differently, and this will be reported independently.

Reaction of **1** with furan-d_4 yielded [Cp_2Zr(*c*-C_3H_4D)(2-C_4D_3O)] (**3-*d*$_4$**). In addition to a deuterated furyl group, selective incorporation of one deuterium in one of the equivalent *β′* positions on the same enantioface of the cyclopropyl group as the zirconium was inferred from ^{1}H (integration of the signal of H*β′* at *δ* −0.03 was half that of H*β* at *δ* −0.45, indicating a change in the multiplicity), ^{2}H (single resonance at *δ* −0.45 in C_6F_6), and ^{13}C NMR spectroscopy (Figure 1 and Scheme 4).

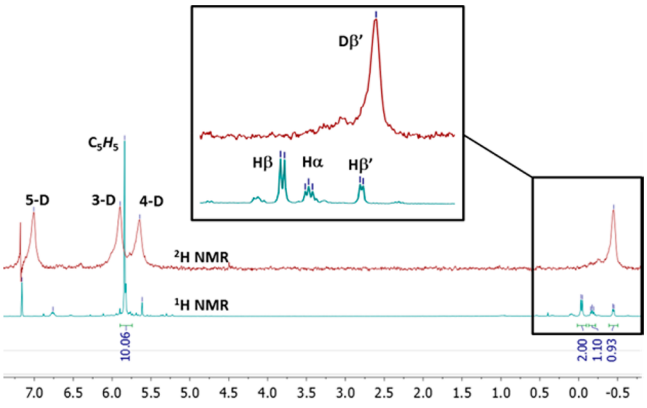

Figure 1. Superimposed ^{1}H (bottom) and ^{2}H (top) NMR spectra of a crude reaction of **1** and furan-d_4 (solvent C_6F_6) to give **3-*d*$_4$**, showing selective D incorporation, with an expansion plot of the high-field region.

Scheme 4. Reaction of Cp_2Zr(*c*-C_3H_5)$_2$ (1) with Furan-d_4

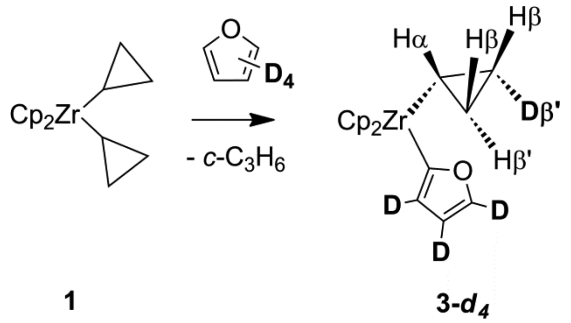

Overall, the synthetic and spectroscopic results are consistent with generation of the unsaturated η^2-cyclopropene intermediate [$Cp_2Zr(\eta^2$-*c*-C_3H_4)] (**A**) by *β*-H abstraction of cyclopropane in **1**, followed by its mechanistic reverse, 1,3-CH/D bond addition across a Zr(η^2-*c*-C_3H_4) bond of **A** (Scheme 5), just like in the Nb case examined previously. **A** has been trapped and functionalized in many ways, but its CH bond activation chemistry has never been described.[57]

Scheme 5. *β*-H Abstraction from 1 Followed by 1,3-CH Bond Activation by Transient A

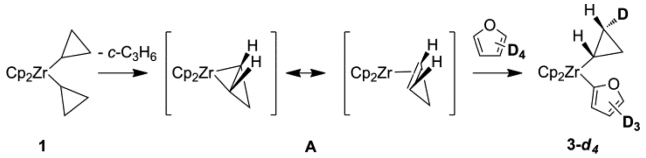

Structural Results. For the purpose of comparison with computational results described below, the X-ray crystal structure of **1** was sought. Among the three independent molecules that were found in the unit cell, only one is not disordered; the second one shows rotational disorder of one Cp ring, whereas the last one shows a more detrimental disorder of one cyclopropyl ring. For the first two cases, and for the non-disordered part of the third one, the geometries are strikingly similar, with only minor differences. A view of the non-disordered complex is shown in Figure 2. Prominent features

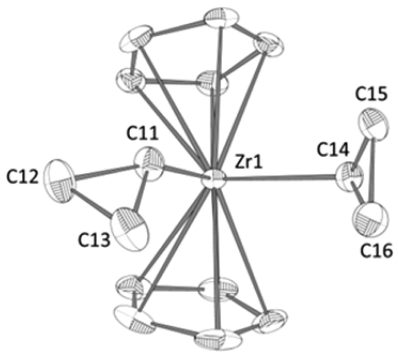

Figure 2. X-ray molecular structure of one of the independent molecules of [Cp_2Zr(*c*-C_3H_5)$_2$] (**1**). Selected bond distances (Å) and angles (deg): Zr(1)−C(11) 2.256(3), Zr(1)−C(14) 2.261(3), C(11)−C(12) 1.498(4), C(11)−C(13) 1.525(4), C(14)−C(16) 1.517(4), C(14)−C(15) 1.524(4); C(11)−Zr(1)−C(14) 97.45(11), C(12)−C(11)−Zr(1) 131.2(2), C(13)−C(11)−Zr(1) 130.6(2), C(16)−C(14)−Zr(1) 119.2(2), C(15)−C(14)−Zr(1) 120.7(2).

include (i) different conformations of the two cyclopropyl groups with respect to the zirconocene moiety, (ii) virtually identical Zr−C*α* and C*α*−C*β* bond distances, and (iii) equal Zr−C*α*−C*β* angles for a given cyclopropyl group, although the values of these angles depend on the conformation of the cyclopropyl rings. The C14-based cyclopropyl ring is virtually perpendicular to the zirconocene plane C(14)−Zr(1)−C(11) (C*α*−Zr−C*α′*), with the C(14)−H bond directed outside. It has Zr−C*α*−C*β* angles of ca. 120°. The C11-based cyclopropyl is oriented in such a way that one C*α*−C*β* bond [namely C(11)−C(12)] is almost coplanar with the zirconocene plane [C(14)−Zr(1)−C(11)−C(12) −162°], with C(12) directed outside. This cyclopropyl ring has Zr−C*α*−C*β* angles of ca. 131°. There is no evidence for any CH or CC agostic distortion.

An X-ray crystal structure of **2** has been obtained (Figure 3). Salient features include (i) the presence of a 2-thienyl group bound to Zr, (ii) the absence of S-coordination, and (iii) the absence of CH or CC agostic distortions of the cyclopropyl group. The planar cyclopropyl and 2-thienyl groups are not perfectly perpendicular to the zirconocene plane [C(1)−Zr(1)−C(5)−C(7) −39.1, C(1)−Zr(1)−C(5)−C(6) 29.7,

dx.doi.org/10.1021/om501056b | *Organometallics* XXXX, XXX, XXX−XXX

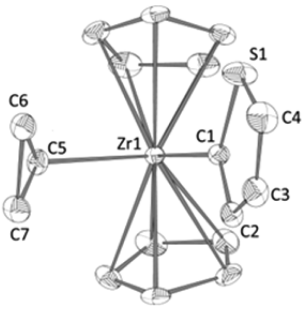

Figure 3. X-ray molecular structure of $[Cp_2Zr(c\text{-}C_3H_5)(2\text{-}C_4H_3S)]$ (**2**). Selected bond distances (Å) and angles (deg): Zr(1)−C(1) 2.2909(18), Zr(1)−C(5) 2.2511(18), C(1)−C(2) 1.412(3), C(2)−C(3) 1.431(3), C(3)−C(4) 1.348(3), C(1)−S(1) 1.7252(18), C(4)−S(1) 1.704(3), C(5)−C(6) 1.515(3), C(5)−C(7) 1.513(3), C(6)−C(7) 1.493(3); C(1)−Zr(1)−C(5) 99.57(7), C(6)−C(5)−Zr(1) 116.70(14), C(7)−C(5)−Zr(1) 122.61(14), C(2)−C(1)−Zr(1) 128.31(13), S(1)−C(1)−Zr(1) 123.18(9).

C(5)−Zr(1)−C(1)−C(2) 74.7, and C(5)−Zr(1)−C(1)−S(1) −88.8°].

Kinetic and Stereochemical Studies. Kinetic studies were conducted in order to probe the mechanism of these C−H bond activation reactions. The reaction of **1** with furan has been investigated in detail. The disappearance of **1** was monitored (with adamantane as an internal standard) by ^{1}H NMR spectroscopy in C_6D_{12} in the presence of 5, 10, 15, and 20 equiv of furan. The corresponding ln([**1**]/[adamantane]) vs time plots (Figure 4) indicate the reaction is first-order in **1** and

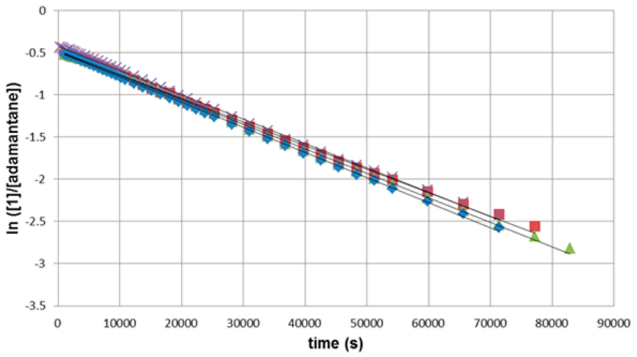

Figure 4. First-order kinetic plots for the disappearance of **1** in the presence of (◆) 5, (■) 10, (▲) 15, and (×) 20 equiv of furan at 323 K.

zeroth-order in furan, with $k_{H,323} = (2.98 \pm 0.09) \times 10^{-5}$ s^{-1} at 323 K over at least three half-lives. In the presence of 15 equiv of furan-d_4, an identical study revealed the absence of isotope effect ($k_{D,323} = (2.93 \pm 0.09) \times 10^{-5}$ s^{-1}; $k_H/k_D = 0.97$) for the disappearance of **1**. Temperature-dependent studies between 313 and 338 K in the presence of 15 equiv of furan (Figure 5) yielded an activation enthalpy of $\Delta H^{\ddagger} = 93 \pm 4$ kJ/mol and a negative activation entropy of $\Delta S^{\ddagger} = -45 \pm 10$ J/K·mol, consistent with some bond breaking in a somewhat ordered transition state. This would correspond to $\Delta G^{\ddagger} = 107 \pm 4$ kJ/mol at 323 K.

Overall, the kinetic results are consistent with a rate-determining intramolecular loss of cyclopropane from **1** by β-H abstraction that generates a reactive unsaturated intermediate **A**, which then activates rapidly and selectively an α-CH bond of furan to give **3** in a 1,3-stereospecific manner (Scheme 6). As

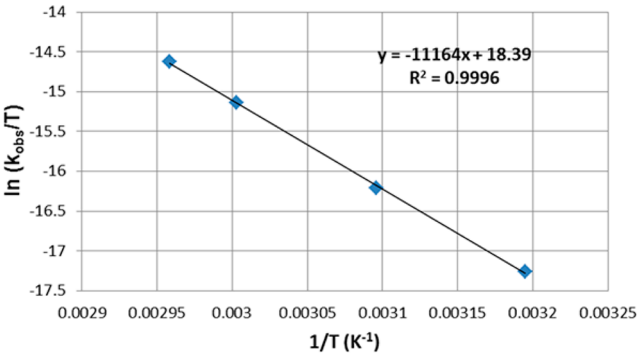

Figure 5. Eyring plot for the reaction of **1** with furan.

Scheme 6. Proposed Pathway for β-H Abstraction/1,3-CH Activation from 1

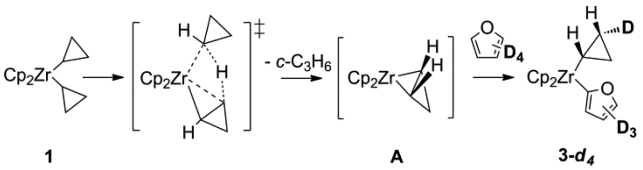

mentioned above, this mechanistic scheme for CH bond formation/activation has rarely been observed when an alkene intermediate is involved. We have reported on the behavior of the niobium cyclopropyl methyl complex $[Tp^{Me_2}NbMe(c\text{-}C_3H_5)(MeCCMe)]$ that activates benzene and alkylaromatic CH bonds via a similar mechanism.[53,54] Obviously, the stability of the η^2-cyclopropene intermediate plays a key role in this chemistry. The generality of this CH bond activation scheme, along with σ-bond metathesis and reversible α-CH abstraction/1,2-addition pathways, is now firmly established.

In order to probe the post-rate-determining CH activation step converting **A** and furan to **3**, we carried out a competition experiment. Thermolysis of **1** in the presence of an excess of a 1:1 mixture of furan and furan-d_4 in cyclohexane-d_{12} at 323 K yielded a mixture of **3** and **3-d_4**, whose ratio led to a kinetic isotope effect (KIE) $k_H/k_D = 2.4 \pm 0.4$ for the discrimination of the C−H versus the C−D bond. Although this value is smaller than that for the reaction of $[Tp^{Me_2}NbMe(c\text{-}C_3H_5)(MeCCMe)]$ with benzene ($k_H/k_D = 4.0 \pm 0.4$), its magnitude suggests that CH/D bond weakening is significant in the transition state for CH/D cleavage.

There are two noticeable differences between the Nb and the Zr systems. First, the niobium complex is known to exhibit an α-CC agostic cyclopropyl group, whereas **1** does not. Second, $\Delta S^{\ddagger}$ is virtually zero in the niobium system, whereas it is markedly negative in the case of **1**. It is tempting to ascribe this difference to the presence of the α-CC agostic distortion that pre-organizes the hydrocarbyl ligands for CH bond abstraction in the case of Nb but not in the case of Zr. This issue and others were addressed with the help of computational studies.

Computational Studies. Computational studies aimed at probing the structural and mechanistic differences between the Zr and Nb cases have been carried out at the DFT PBE1PBE/SDD (Zr)/TZVP (O, C, H) level of theory. Studies on the niobium systems have shown that this functional appropriately describes CH and CC agostic distortions.[63−65] Since reactions were carried out in nonpolar cyclohexane, energies were not corrected for solvent influence. We focused our interest on the β-H abstraction of cyclopropane from **1** leading to intermediate

dx.doi.org/10.1021/om501056b | Organometallics XXXX, XXX, XXX−XXX

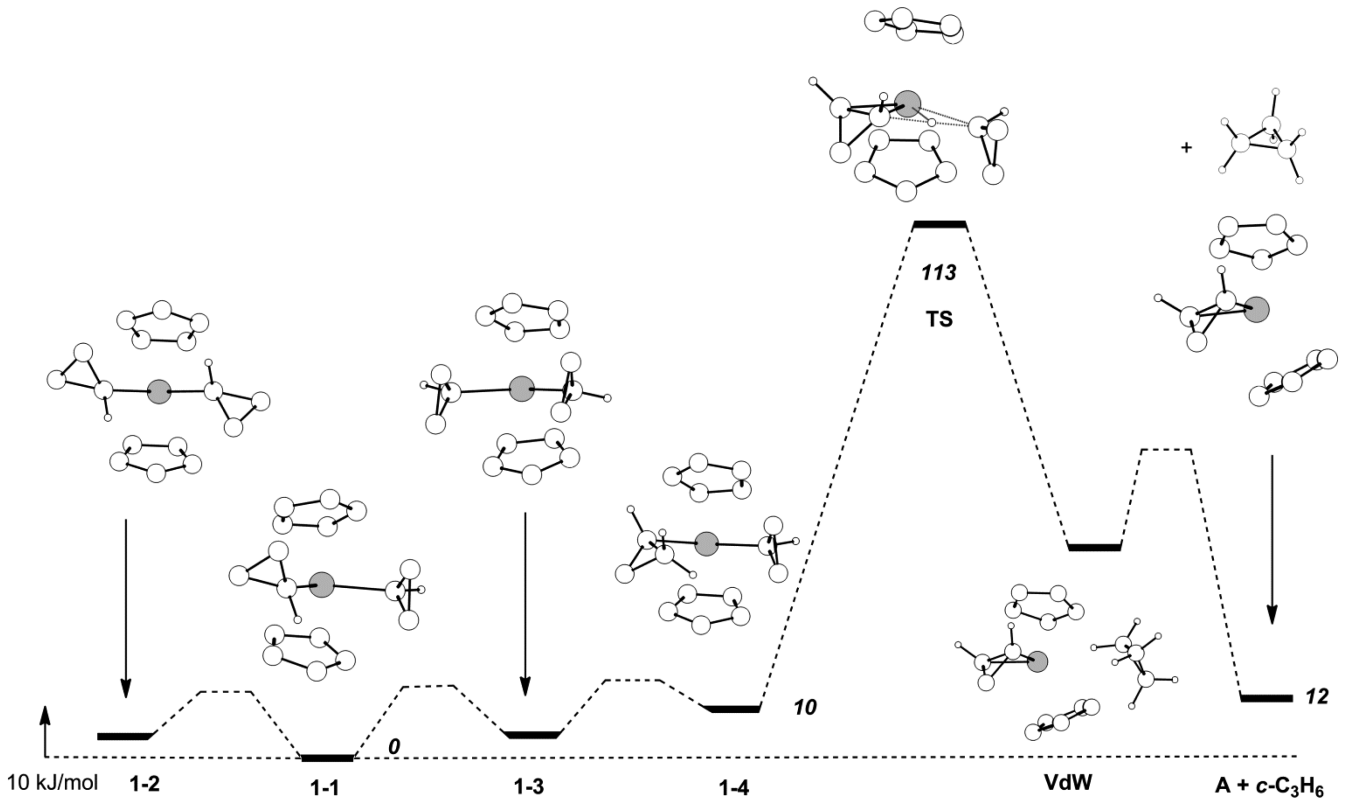

Figure 6. Computed Gibbs energy (kJ/mol) profile for the β-H abstraction of cyclopropane from **1**, giving intermediate **A** (Zr, gray; C and H, white spheres).

A, the rate-determining step of the whole process. The computed energy profile for this step is depicted in Figure 6.

Three rotamers of **1**, namely **1-1**, **1-2**, and **1-3**, were computed within a 6 kJ/mol energy range. No efforts were invested in finding the rotational barriers. The more stable rotamer **1-1** exhibits cyclopropyl groups that have conformations almost identical to those in the X-ray crystal structure of **1**; the computed metrical parameters of **1-1** reproduce well those of **1**, confirming the appropriate choice of the method (Figure 7).

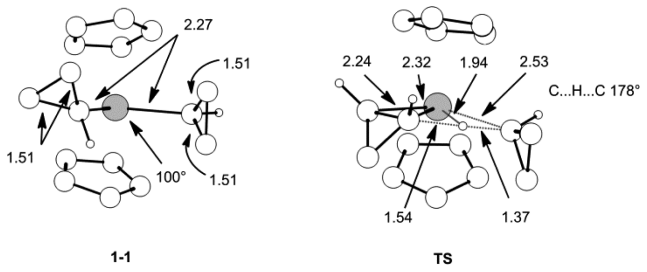

Figure 7. DFT-optimized structures of **1-1** (left), the most stable rotamer of **1**, and of **TS** (right), the transition state for β-H abstraction of cyclopropane (bond lengths in Å; Zr, gray; C and H, white spheres).

The transition state **TS** for β-H abstraction is 113 kJ/mol above **1-1**, in accord with a reaction occurring readily above room temperature. This value is moreover in good agreement with the experimental value of $\Delta G^{\ddagger}$ = 107 ± 4 kJ/mol (see above). **TS** has a typical σ-bond metathesis type of geometry (Figure 7), with a linear (C···H···C 178°) transfer of a β-H$^+$ (natural charge, NC = +0.27) between the β-carbon (NC = −0.52) of a cyclopropyl group, which will give the η^2-*c*-C_3H_4, and the α-carbon (NC = −0.53) of the other, which will give cyclopropane. **TS** is a late transition state in the sense that it is not symmetrical—CH bond-breaking is 1.54 Å, whereas CH bond-forming is 1.37 Å—and there are incipient η^2-cyclopropene and cyclopropane fragments. The hydrogen transfer seems to be assisted by the zirconium, with a Zr···H distance of 1.94 Å. The geometry and energy of **TS** are similar to those computed for the β-H abstraction of methane in the niobium complex [Tp^{Me_2}NbMe(*c*-C_3H_5)(MeCCMe)], which yields the same type of η^2-cyclopropene intermediate, [Tp^{Me_2}Nb(η^2-*c*-C_3H_4)(MeCCMe)]. Relaxation of **TS** on the product side yields the η^2-cyclopropene [$Cp_2Zr(\eta^2$-*c*-C_3H_4)] intermediate **A** and cyclopropane via a van der Waals complex **VdW**. On the reactant side, remarkably, none of the previously optimized rotamers of **1** is obtained. Instead, rotamer **1-4**, which exhibits one distorted cyclopropyl group, is found (Figure 6). Rotamer **1-4** sits only 10 kJ/mol higher than the most stable rotamer, **1-1**.

Most prominently, **1-4** exhibits clear signs of α-CC agostic distortion for one of the cyclopropyl groups (Figure 8). A reduced Zr−Cα−Cβ angle (100°) for the CC bond that sits approximately in the Cα−Zr−Cα' plane is accompanied by a remarkably long Cα−Cβ bond (1.54 Å) as compared to the non-agostic one (1.50 Å). The latter is marginally shorter than those in the undistorted cyclopropyl groups in all the rotamers. Further evidence for the interaction comes from the computed carbon−carbon NMR coupling constants, J_{CC}. We have shown that this computation is very reliable not only to give trends in the variation of coupling constants but also to yield meaningful absolute values.[55] Taking the undistorted cyclopropyl group in **1-4** as a reference, with $J_{C\alpha C\beta}$ = 6.1 and 8.3 Hz, a significantly

dx.doi.org/10.1021/om501056b | *Organometallics* XXXX, XXX, XXX−XXX

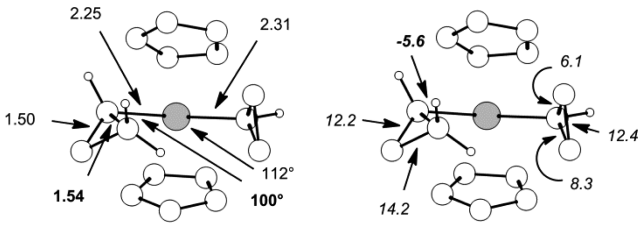

Figure 8. Rotamer **1-4**: (left) relaxation of the transition state for cyclopropane elimination with metrical parameters (bond lengths in Å), and (right) computed NMR coupling constants (J_{CC} in Hz) (Zr, gray; C and H, white spheres).

reduced $J_{C\alpha C\beta}$ = −5.6 Hz is computed for the elongated α-agostic CC bond, whereas an increased value of $J_{C\alpha C\beta}$ = 12.2 Hz characterizes the other CαCβ bond. Similar values have been measured and/or computed for group 3 (Y) and group 5 (Nb) α-CC agostic complexes.[53,66] There is no evidence for an accompanying CH agostic distortion (β-CH = 1.088, 1.084 Å; J_{CH} = 142, 156 Hz, respectively). Computation of methane elimination from [$Cp_2ZrMe(c\text{-}C_3H_5)$] yielded a potential energy surface very similar to the one just described, with again an α-CC agostic intermediate located on the way to β-H abstraction (see SI).

We now can see the importance of the α-CC agostic distortion in these systems based on cyclopropyl groups. In the niobium system, where the most stable structure is α-CC agostic, the entropy of activation is close to zero, suggesting the agostic interaction prepares the β-CH bond abstraction step. In the zirconium case, the entropy of activation is markedly negative because of a larger difference in organization between non-agostic **1** and **TS**. Remarkably, the computed entropy difference between the non-agostic and agostic rotamers of the zirconium system, **1-1** and **1-4**, respectively, is −16 J/mol·K, confirming the connection between agosticity and entropy. The α-CC agostic assistance for β-H abstraction is reminiscent of the β-CH agostic assistance for β-H abstraction of an alkane from [Cp_2ZrRR'] (R, R′ = various alkyls) that leads to unsaturated reactive η^2-alkene intermediates [$Cp_2Zr(\eta^2$-alkene)], as suggested by Negishi[52,67] and Buchwald.[68] As far as we are aware, though, none of these complexes promote CH bond activation of simple hydrocarbons. Terminal alkynes having more reactive CH bonds react with η^2-alkene titanocenes or zirconocenes to give alkyl alkynyl derivatives.[47,48] A stable η^2-isobutylene hafnocene complex generated from an *n*-butyl *tert*-butyl complex via β-H abstraction activates benzene by a 1,3-addition pathway at higher temperature (70 °C).[46] Hence, CH bond activation in these complexes appears to be favorable if the interaction between the transition metal fragment and the alkene is strong enough to provide a stable transient complex and/or the activated CH bond is reactive enough. The strained cyclopropene is unique is this respect.

Another difference between the Zr and Nb cases is the magnitude of the KIE for the cleavage of the CH/CD bond of furan by **A** (k_H/k_D = 2.4) and that of benzene by [$Tp^{Me_2}NbMe(\eta^2\text{-}c\text{-}C_3H_4)$(MeCCMe)] (**A′**) ($k_H/k_D$ = 4.0). The computed geometry of the transition state for the 1,3-CH bond cleavage of furan by **A** is shown Figure 9, where it is compared with the Nb case.[53] While an almost linear C···H···C σ-bond metathesis type of arrangement is observed in the two cases, the CH bond of furan is not elongated as much

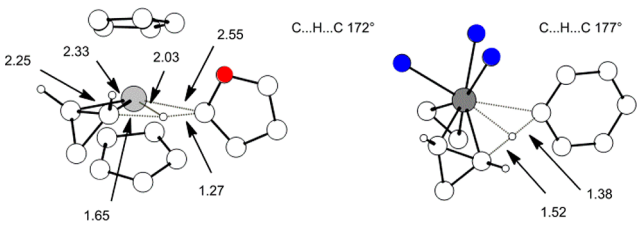

Figure 9. DFT-optimized transition-state structures for CH bond cleavage of (left) furan by **A** and (right) benzene by [$Tp^{Me_2}NbMe(\eta^2\text{-}c\text{-}C_3H_4)$(MeCCMe)] (**A′**); distances in Å (Zr, gray; Nb, dark gray; C and H, white; O, red; N, blue spheres). For **A′**, only atoms of ancillary ligands directly bound to Nb are shown for clarity.

as that of benzene in the two transition states. This earlier, less symmetrical transition state in the Zr case is fully consistent with the smaller experimental KIE observed for the CH cleavage event. Computation of the KIE for the CH/D activation of furan by **A** yielded $\Delta G^{\ddagger}$ = 78 and 81 kJ/mol (at 298 K), respectively, translating to k_H/k_D = 3.3 at this temperature. Similar calculations for the CH/D activation of benzene in the niobium case gave k_H/k_D = 4.0 ($\Delta G^{\ddagger}$ = 120 vs 123.5 kJ/mol for C_6H_6 vs C_6D_6). The agreement with the experimental results is excellent, confirming the correctness of the model and our understanding of the system.

Nature of the α-CC Agostic Interaction. We have probed the nature of the α-CC agostic interaction in **1-4** with the help of a natural population analysis (NPA) and natural bond orbital (NBO) analysis.[69] Typical second-order interactions involving the σ and σ*-CC NBOs of the cyclopropyl group provide an internal benchmark (18−22 kJ/mol range for the present model). A conspicuous interaction (38 kJ/mol) involving the C−C NBO and an empty Zr-based 3d orbital characterizes the α-CC agostic interaction. This interaction is clearly seen in the NLMO in Figure 10, with 3.4% d character.

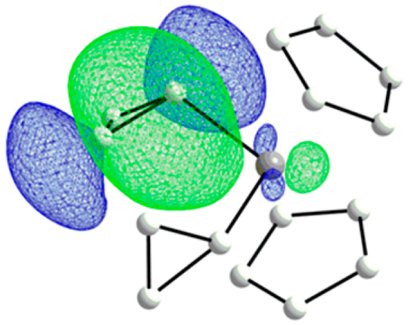

Figure 10. NLMO describing the α-CC interaction in **1-4**.

All four β-carbons, whether agostic or not, bear the same natural charge (NC = −0.42 to −0.43), emphasizing the covalent nature of the interaction. There is no evidence of interaction between any of the cyclopropyl CH bonds and Zr that could be ascribed to a CH agostic interaction. These interactions appear weaker than in the bis(agostic) complex [$Cp^*_2Y(\mu\text{-}c\text{-}C_3H_5)_2Li$(thf)], for which an additional CHY agostic interaction was seen.[66]

CONCLUSIONS

η^2-Alkene complexes of the early transition metals are capable of activating CH bonds of various hydrocarbons; i.e., the reaction is quite general. It appears that the strained three-

dx.doi.org/10.1021/om501056b | *Organometallics* XXXX, XXX, XXX−XXX

membered ring in the group 4 and 5 transition metal complexes plays a dual role in stabilizing the key η^2-alkene intermediate and in providing α-CC agostic interactions along the reaction coordinate. Intramolecular CC bond cleavage is precluded for these high oxidation state metals, and the α-CC agostic distortion orients and prepares the intramolecular β-H abstraction.

EXPERIMENTAL SECTION

General Considerations. All air- and moisture-sensitive compounds were handled using vacuum line, Schlenk, and cannula techniques, or in a JACOMEX GP-Concept glovebox under an argon atmosphere. Solvents were dried and distilled using the conventional methods by Na/benzophenone (diethyl ether, tetrahydrofuran), Na (toluene), or CaH_2 (dichloromethane, cyclohexane, pentane) or passed on activated alumina columns and then degassed by freeze−pump−thaw cycles. C_6F_6, thiophene, furan, and deuterated solvents and reactants (benzene-d_6, cyclohexane-d_{12}, furan-d_4) were degassed by freeze−pump−thaw cycles, dried over molecular sieves, and stored under argon. Commercial $[Cp_2ZrCl_2]$ was recrystallized from dichloromethane. The synthesis of complex **1** was carried out by a modification of the reported procedure[58] and fully characterized. Cyclopropyllithium was prepared according to a literature procedure.[70] ^{1}H, ^{13}C, and ROESY NMR spectra were obtained using Bruker DPX300 or AVANCE 300, 400, or 500 spectrometers at room temperature unless otherwise stated. Chemical shifts are given in ppm downfield from Me_4Si, using residual proton (C_6D_5H, δ 7.16; C_7D_7H, δ 2.08; $C_6D_{11}H$, δ 1.42) or carbon (C_6D_6, δ 128.39; C_7D_8, δ 20.43) signals of the deuterated solvents.

Synthesis of Dicyclopropyl Zirconocene [$Cp_2Zr(c\text{-}C_3H_5)_2$] (1). In a glovebox, $[Cp_2ZrCl_2]$ (700 mg, 2.40 mmol) and cyclopropyllithium (25% by weight, 920 mg, 4.79 mmol) were dissolved in 15 mL of toluene and stirred at room temperature for 2 h, during which time the colorless solution turned yellow. The solvent was removed under vacuum, and the resulting solid was extracted with pentane and filtered to give a clear yellow solution. After evaporation of the solvent, the solid was crystallized from cold pentane to yield **1** as a yellow crystalline solid that was stored below 0 °C (620 mg, 2.04 mmol, 85%). ^{1}H NMR (500.3 MHz, toluene-d_8, 233 K): δ 5.59 (s, 10 H, η^5-C_5H_5), 0.78 (dd, 4 H, J = 10.0, 1.4 Hz, c-C_3H_5 β), 0.42 (dd, 4 H, J = 7.9, 1.4 Hz, c-C_3H_5 β'), −0.18 (m, 2H, c-C_3H_5 α). ^{13}C NMR (125.8 MHz, toluene-d_8, 233 K): δ 109.8 (d, J_{CH} = 172 Hz, η^5-C_5H_5), 33.9 (d, J_{CH} = 133 Hz, c-C_3H_5 α), 10.20 (t, J_{CH} = 158 Hz, c-C_3H_5 β).

Synthesis of Cyclopropyl(2-thienyl)zirconocene [$Cp_2Zr(c\text{-}C_3H_5)(2\text{-}C_4H_3S)$] (2). **1** (200 mg, 0.66 mmol) was dissolved in 12 mL of cyclohexane, and thiophene (0.53 mL, 6.6 mmol) was added. The mixture was heated at 60 °C for 24 h to give an orange solution. The solvent was removed under reduced pressure, and the residue was extracted with pentane. After evaporation of the solvent, the solid was crystallized from cold pentane to yield **2** as a yellow crystalline solid, which was stored at −40 °C (150 mg, 0.44 mmol, 66%). Anal. Calcd for $C_{17}H_{18}SZr$: C, 59.08; H, 5.21. Found: C, 59.15; H, 4.78. ^{1}H NMR (400.1 MHz, cyclohexane-d_{12}, 298 K): δ 7.35, (dd, 1 H, J = 4.4, 0.7 Hz, 5-H-C_3H_3S), 7.02 (dd, 1 H, J = 3.2, 0.7 Hz, 3-H-C_3H_3S), 6.91 (dd, 1 H, J = 4.4, 3.2 Hz, 4-H-C_3H_3S), 6.11 (s, 10 H, η^5-C_5H_5), 0.56 (dd, 2 H, J = 9.8, 1.6 Hz, c-C_3H_5 β), 0.26 (dd, 2 H, J = 8.2, 1.6 Hz, c-C_3H_5 β'), 0.13 (m, 1H, c-C_3H_5 α). ^{13}C NMR (100.6 MHz, benzene-d_6, 298 K): δ 176.7 (dd, J_{CH} = 15, 8 Hz, 2-c-C_3H_3S), 137.2 (ddd, J_{CH} = 162, 11, 6 Hz, 5-c-C_3H_3S), 130.8 (dt, J_{CH} = 182, 9 Hz, 4-c-C_3H_3S), 127.1 (ddd, J_{CH} = 163, 8, 5 Hz, 3-c-C_3H_3S), 110.7 (d, $^1J_{CH}$ = 174 Hz, η^5-C_5H_5), 41.2 (d, J_{CH} = 135 Hz, c-C_3H_5 α), 11.3 (t, J_{CH} = 159 Hz, c-C_3H_5 β).

Synthesis of Cyclopropyl(2-furyl)zirconocene [$Cp_2Zr(c\text{-}C_3H_5)(2\text{-}C_4H_3O)$] (3). Following a procedure similar to that for **2**, reaction between **1** (200 mg, 0.66 mmol) and furan (0.50 mL, 6.6 mmol) yielded **3** as a yellow crystalline solid (140 mg, 0.42 mmol, 65%). The reaction can be carried out in C_6F_6 with similar results. Anal. Calcd for $C_{17}H_{18}OZr$: C, 61.96; H, 5.47. Found: C, 61.57; H, 5.46. ^{1}H NMR (400.1 MHz, cyclohexane-d_{12}, 298 K): δ 7.41 (dd, 1 H, J = 1.6, 0.6 Hz, 5-H-C_3H_3O), 6.28 (dd, 1 H, J = 3.1, 0.6 Hz, 3-H-C_3H_3O), 6.09 (dd, 1 H, J = 3.1, 1.6 Hz, 4-H-C_3H_3O), 6.05 (s, 10 H, η^5-C_5H_5), 0.46 (dd, 2 H, J = 9.6, 2.2 Hz, c-C_3H_5 β), 0.29 (m, 1 H, c-C_3H_5 α), 0.16 (dd, 2 H, J = 7.9, 2.2 Hz, c-C_3H_5 β'). ^{13}C NMR (100.6 MHz, benzene-d_6, 298 K): δ 202.9 (dd, J_{CH} = 15, 5 Hz, 2-c-C_3H_3O), 144.5 (ddd, J_{CH} = 196, 12, 6 Hz, 5-c-C_3H_3O), 123.9 (ddd, J_{CH} = 169, 6, 4 Hz, 4-c-C_3H_3O), 109.8 (d, J_{CH} = 173 Hz, η^5-C_5H_5), 108.5 (ddd, J_{CH} = 171, 15, 5 Hz, 2-c-C_3H_3O), 41.3 (d, J_{CH} = 139 Hz, c-C_3H_5 α), 9.8 (t, J_{CH} = 161 Hz, c-C_3H_5 β).

Synthesis of (2-*d*-Cyclopropyl)(3,4,5-d_3-2-furyl)zirconocene [$Cp_2Zr(c\text{-}C_3H_4D)(2\text{-}C_4D_3O)$] (3-$d_4$). **1** (10 mg, 0.032 mmol) was dissolved in 0.6 mL of hexafluorobenzene in a Young-type NMR tube, and furan-d_4 (0.04 mL, 0.8 mmol) was added. The mixture was heated at 60 °C for 24 h to give a yellow solution. The solvent was removed under reduced pressure, and the residue was extracted with pentane. After evaporation of the solvent, **3-d_4** was obtained as a yellow crystalline solid. ^{1}H NMR (500.1 MHz, C_6F_6 with benzene-d_6 capillary, 298 K): δ 5.84 (s, 10 H, η^5-C_5H_5), −0.04 (d, 2 H, J_{HH} = 10.2, c-C_3H_4D β), −0.17 (m, 1H, c-C_3H_4D α), −0.46 (d, 1 H, J_{HH} = 7.8, 2.2 Hz, c-C_3H_4D β'). ^{2}H{^{1}H} NMR (76.8 MHz, C_6F_6 with benzene-d_6 capillary, 298 K): δ 7.0 (s, 5-D-C_3D_3O), 5.89 (s, 3-D-C_3D_3O), 5.64 (s, 4-D-C_3H_3O), −0.46 (s, c-C_3H_4D β'). ^{13}C{^{1}H}{^{2}H} NMR (100.6 MHz, cyclohexane with benzene-d_6 capillary, 298 K): δ 109.54 (s, η^5-C_5H_5), 40.39 (s, c-C_3H_4D, $C\alpha$H), 9.04 (s, c-C_3H_4D, $C\beta H_2$), 8.98 (t, J_{CD} = 24 Hz, c-C_3H_4D, $C\beta$HD); C_3D_3O signals not observed.

Kinetics of the Reaction between 1 and Furan. In a Young-type 5 mm NMR tube in the glovebox, **1** (40 mg, 0.13 mmol) was dissolved in 0.5 mL of cyclohexane-d_{12} containing adamantane (16 mg, 0.12 mmol) as an internal standard. The appropriate amount of furan (5, 10, 15, or 20 equiv) was then added with a microsyringe. The tube was then introduced in the preheated NMR probe at a given temperature. Acquisitions of ^{1}H NMR spectra started 10 min later to allow temperature equilibration. Each acquisition was composed of eight scans with a 1 s delay between scans (total acquisition time 2 min). Reaction progress (disappearance of **1**) was automatically monitored at given intervals by ^{1}H NMR during at least three half-lifes by integration of the cyclopentadienyl singlet of **1** at δ 5.79 with respect to the two adamantane singlets at δ 1.86 and 1.78. From the corresponding ln([**1**]/[adamantane]) vs time plots, the reaction was found to be first-order in **1** and zeroth-order in furan, with k_{obs} = (2.98 ± 0.09) × 10^{-5} s^{-1} at 323 K. An Eyring analysis was similarly carried out at four different temperatures between 313 and 338 K, and the following rate constants were obtained: k_{obs} = 9.67 × 10^{-6} s^{-1} (313 K), 2.98 × 10^{-5} s^{-1} (323 K), 8.33 × 10^{-5} s^{-1} (333 K), and 1.50 × 10^{-4} s^{-1} (338 K). The Erying plot for these k values (ln(k/T) vs T^{-1}) gave the activation parameters $\Delta H^{\ddagger}$ = 93 ± 4 kJ/mol and $\Delta S^{\ddagger}$ = −45 ± 10 J/K·mol.

Kinetics of the Reaction between 1 and Furan-d_4. Following a procedure similar to that for the reaction with furan, **1** (40 mg, 0.13 mmol) was reacted with 15 equiv of furan-d_4 in 0.5 mL of cyclohexane-d_{12} in the presence of adamantane (16 mg, 0.11 mmol). The tube was then placed in the preheated NMR probe at 323 K, and automatic acquisitions of ^{1}H NMR spectra started 10 min later to allow temperature equilibration. Data treatment resulted in a linear ln([**1**]/[adamantane]) vs time plot with k_{obs} = (2.93 ± 0.09) × 10^{-5} s^{-1} at 323 K, from which k_H/k_D = 1.0 was obtained.

Competition Experiment between 1 and a Mixture of Furan and Furan-d_4. Following a procedure similar to that for the reaction with furan, **1** (41.0 mg, 0.132 mmol) was reacted with an excess of a furan:furan-d_4 mixture (1:1 by vol, 0.070 mL of each) in 0.6 mL of cyclohexane-d_{12} in the presence of adamantane (16.8 mg, 0.12 mmol). The tube was then placed in the preheated NMR probe at 323 K, and automatic acquisitions of ^{1}H NMR spectra started 10 min later to allow temperature equilibration. Integration (acquisition time + 30 s delay between pulses to ensure complete relaxation) of the furyl versus the cyclopentadienyl signals at 298 K on the crude reaction mixture after completion of the reaction or in benzene-d_6 after removal of volatiles yielded an identical k_H/k_D = 2.4 ± 0.4. Measurements at the temperature of the experiment and after different reaction times

dx.doi.org/10.1021/om501056b | Organometallics XXXX, XXX, XXX−XXX

yielded identical results, indicating the reverse reaction was not kinetically significant.

X-ray Crystallography. Data for **1** and **2** were collected at 180 K on a Bruker Apex II diffractometer using graphite-monochromated Mo Kα radiation (λ = 0.71073 Å) and equipped with an Oxford Cryosystems Cryostream Cooler Device. The structures were solved by direct methods and refined by means of least-squares procedures on F^2 with the aid of the program SHELX-L97[71] included in the software package WinGX version 1.63.[72] All non-hydrogen atoms were anisotropically refined. All hydrogen atoms were refined by using a riding model. For **1**, the asymmetric unit contains three independent molecules. Two of those molecules are disordered: one involves rotational disorder of an η^5-C_5H_5 ring, and the other involves one cyclopropyl group. Both disorders have been treated in SHELXL using the PART command. Refinement of the final model led to an imperfect but reasonable solution. One alert level B resulting from the disorder remained (ratio of maximum/minimum residual density). Full crystallographic details can be obtained free of charge from the Cambridge Crystallographic Data Center via www.ccdc.cam.ac.uk/data_request/cif (CCDC 1022288 and CCDC 1022289 for **2** and **1**, respectively). For **1**: colorless crystal, $C_{16}H_{20}Zr$, FW 303.54 g/mol, trigonal, $P\bar{3}$, a = 23.4826(6), b = 23.4826(6), and c = 13.0911(4) Å, V = 6251.7(4) Å^3, T = 180(2) K, Z = 18, data/restraints/parameters 7654/270/533; final R indices [$I > 2\sigma(I)$] R_1 = 0.0254, wR_2 = 0.0650; R indices (all data) R_1 = 0.0283, wR_2 = 0.0678; goodness-of-fit on F^2 = 1.066. For **2**: light yellow crystal, $C_{17}H_{18}SZr$, FW 345.59 g/mol, monoclinic, $P2_1/c$, a = 13.0228(6), b = 8.2073(4), and c = 14.8470(7) Å, β = 111.593(2)°, V = 1475.51(12) Å^3, T = 180(2) K, Z = 4, data/restraints/parameters 5089/0/172; final R indices [$I > 2\sigma(I)$] R_1 = 0.0289, wR_2 = 0.0688; R indices (all data) R_1 = 0.0384, wR_2 = 0.0738; goodness-of-fit on F^2 = 1.035.

Computational Details. Calculations were performed at the DFT level with the PBE1PBE functional[73] as implemented in Gaussian03, revision E.01.[74] Zr was described using the Stuttgart/Dresden RECP (SDD) pseudopotential and its associated basis set.[75] For O, C, and H, the TZVP basis set was used.[75] Structure optimizations were carried out without symmetry constraints. The nature of the stationary points was ascertained by a vibrational analysis within the harmonic approximation (1 atm and 298 K). Minima were identified by a full set of real frequencies and transitions states by the presence of a single imaginary frequency. Transitions states were relaxed on both reactant and product sides. Since reactions were carried out in nonpolar cyclohexane, solvent corrections were deemed not necessary. Computation of NMR coupling constants used the same functional associated with the IGLO-II basis set for C and H.[76] NBO calculations[69] were carried out with NBO 5.0 as implemented in Gaussian 03.

■ ASSOCIATED CONTENT

Supporting Information

Representative NMR spectra of complexes, kinetic data, and computational details including a text file of all computed molecule Cartesian coordinates in a format for convenient visualization, and complete ref 74. This material is available free of charge via the Internet at http://pubs.acs.org.

■ AUTHOR INFORMATION

Corresponding Author

*E-mail: michel.etienne@lcc-toulouse.fr.

Notes

The authors declare no competing financial interest.

■ ACKNOWLEDGMENTS

We thank the ANR for partial support of this work (GreenLake project, ANR 11-BS07-009-01).

■ REFERENCES

(1) See the special issue: *Chem. Soc. Rev.* **2011**, *40* (No. 4).
(2) See the special issue: *Acc. Chem. Res.* **2012**, *45* (No. 6).
(3) See the special issue: *Chem. Rev.* **2010**, *110* (No. 2).
(4) Jiao, Y.; Brennessel, W. W.; Jones, W. D. *Chem. Sci.* **2014**, *5*, 804−812.
(5) Jiao, Y.; Morris, J.; Brennessel, W. W.; Jones, W. D. *J. Am. Chem. Soc.* **2013**, *135*, 16198−16212.
(6) Jiao, Y.; Evans, M. E.; Morris, J.; Brennessel, W. W.; Jones, W. D. *J. Am. Chem. Soc.* **2013**, *135*, 6994−7004.
(7) Caballero, A.; Perez, P. J. *Chem. Soc. Rev.* **2013**, *42*, 8809−8820.
(8) Cavaliere, V. N.; Mindiola, D. J. *Chem. Sci.* **2012**, *3*, 3356−3365.
(9) Bergman, R. G. *Nature* **2007**, *446*, 391−393.
(10) Labinger, J. A.; Bercaw, J. E. *Nature* **2002**, *417*, 507−514.
(11) Stahl, S. S.; Labinger, J. A.; Bercaw, J. E. *Angew. Chem., Int. Ed.* **1998**, *37*, 2181−2192.
(12) Arndtsen, B. A.; Bergman, R. G.; Mobley, T. A.; Peterson, T. H. *Acc. Chem. Res.* **1995**, *28*, 154−162.
(13) Boutadla, Y.; Davies, D. L.; Macgregor, S. A.; Poblador-Bahamonde, A. I. *Dalton Trans.* **2009**, 5820−5831.
(14) Lapointe, D.; Fagnou, K. *Chem. Lett.* **2010**, *39*, 1119−1126.
(15) Perutz, R. N.; Sabo-Etienne, S. *Angew. Chem., Int. Ed.* **2007**, *46*, 2578−2592.
(16) Webb, J. R.; Burgess, S. A.; Cundari, T. R.; Gunnoe, T. B. *Dalton Trans.* **2013**, *42*, 16646−16665.
(17) Waterman, R. *Organometallics* **2013**, *32*, 7249−7263.
(18) Sadow, A. D.; Tilley, T. D. *J. Am. Chem. Soc.* **2005**, *127*, 643−656.
(19) Thompson, M. E.; Baxter, S. M.; Bulls, A. R.; Burger, B. J.; Nolan, M. C.; Santarsiero, B. D.; Schaefer, W. P.; Bercaw, J. E. *J. Am. Chem. Soc.* **1987**, *109*, 203−219.
(20) Watson, P. L. *J. Am. Chem. Soc.* **1983**, *105*, 6491−6493.
(21) Wicker, B. F.; Fan, H.; Hickey, A. K.; Crestani, M. G.; Scott, J.; Pink, M.; Mindiola, D. J. *J. Am. Chem. Soc.* **2012**, *134*, 20081−20096.
(22) Royo, P.; Sanchez-Nieves, J. *J. Organomet. Chem.* **2000**, *597*, 61−68.
(23) Schafer, D. F.; Wolczanski, P. T. *J. Am. Chem. Soc.* **1998**, *120*, 4881−4882.
(24) Bennett, J. L.; Wolczanski, P. T. *J. Am. Chem. Soc.* **1997**, *119*, 10696−10719.
(25) Schaller, C. P.; Cummins, C. C.; Wolczanski, P. T. *J. Am. Chem. Soc.* **1996**, *118*, 591−611.
(26) De With, J.; Horton, A. *Angew. Chem., Int. Ed. Engl.* **1993**, *32*, 903−905.
(27) Cummins, C.; Baxter, S.; Wolczanski, P. *J. Am. Chem. Soc.* **1988**, *110*, 8731−8733.
(28) Walsh, P.; Hollander, F.; Bergman, R. *J. Am. Chem. Soc.* **1988**, *110*, 8729−8731.
(29) Zhang, S.; Tamm, M.; Nomura, K. *Organometallics* **2011**, *30*, 2712−2720.
(30) Andino, J. G.; Kilgore, U. J.; Pink, M.; Ozarowski, A.; Krzystek, J.; Telser, J.; Baik, M.-H.; Mindiola, D. J. *Chem. Sci.* **2010**, *1*, 351−356.
(31) Wada, K.; Pamplin, C. B.; Legzdins, P.; Patrick, B. O.; Tsyba, I.; Bau, R. *J. Am. Chem. Soc.* **2003**, *125*, 7035−7048.
(32) Coles, M. P.; Gibson, V. C.; Clegg, W.; Elsegood, M. R. J.; Porrelli, P. A. *Chem. Commun.* **1996**, 1963−1964.
(33) Van der Heijden, H.; Hessen, B. *J. Chem. Soc., Chem. Commun.* **1995**, 145−146.
(34) Flores, J. A.; Cavaliere, V. N.; Buck, D.; Pinter, B.; Chen, G.; Crestani, M. G.; Baik, M.-H.; Mindiola, D. J. *Chem. Sci.* **2011**, *2*, 1457−1462.
(35) Bailey, B. C.; Fan, H.; Huffman, J. C.; Baik, M.-H.; Mindiola, D. J. *J. Am. Chem. Soc.* **2007**, *129*, 8781−8793.
(36) Bailey, B. C.; Fan, H. J.; Baum, E. W.; Huffman, J. C.; Baik, M. H.; Mindiola, D. J. *J. Am. Chem. Soc.* **2005**, *127*, 16016−16017.
(37) Erker, G. *J. Organomet. Chem.* **1977**, *134*, 189−202.
(38) Pamplin, C. B.; Legzdins, P. *Acc. Chem. Res.* **2003**, *36*, 223−233.
(39) Debad, D.; Legzdins, P.; Lumb, S. A.; Rettig, S. J.; Batchelor, R. J.; Einstein, F. W. B. *Organometallics* **1999**, *18*, 3414−3428.

(40) Debad, J.; Legzdins, P.; Lumb, S.; Batchelor, R.; Einstein, F. *J. Am. Chem. Soc.* **1995**, *117*, 3288−3289.
(41) Maron, L.; Perrin, L.; Eisenstein, O. *J. Chem. Soc., Dalton Trans.* **2002**, 534−539.
(42) Baillie, R. A.; Legzdins, P. *Acc. Chem. Res.* **2014**, *47*, 330−340.
(43) Baillie, R. A.; Man, R. W. Y.; Shree, M. V.; Chow, C.; Thibault, M. E.; McNeil, W. S.; Legzdins, P. *Organometallics* **2011**, *30*, 6201−6217.
(44) Tsang, J. Y. K.; Buschhaus, M. S. A.; Graham, P. M.; Semiao, C. J.; Semproni, S. P.; Kim, S. J.; Legzdins, P. *J. Am. Chem. Soc.* **2008**, *130*, 3652−3663.
(45) Ng, S. H. K.; Adams, C. S.; Hayton, T. W.; Legzdins, P.; Patrick, B. O. *J. Am. Chem. Soc.* **2003**, *125*, 15210−15223.
(46) Buchwald, S. L.; Kreutzer, K. A.; Fisher, R. A. *J. Am. Chem. Soc.* **1990**, *112*, 4600−4601.
(47) Cohen, S. A.; Bercaw, J. E. *Organometallics* **1985**, *4*, 1006−1014.
(48) Kissounko, D.; Epshteyn, A.; Fettinger, J. C.; Sita, L. R. *Organometallics* **2006**, *25*, 531−535.
(49) Wang, S. Y. S.; Abboud, K. A.; Boncella, J. M. *J. Am. Chem. Soc.* **1997**, *119*, 11990−11991.
(50) Cavaliere, V. N.; Crestani, M. G.; Pinter, B.; Pink, M.; Chen, C.-H.; Baik, M.-H.; Mindiola, D. J. *J. Am. Chem. Soc.* **2011**, *133*, 10700−10703.
(51) Hirsekorn, K. F.; Veige, A. S.; Marshak, M. P.; Koldobskaya, Y.; Wolczanski, P. T.; Cundari, T. R.; Lobkovsky, E. B. *J. Am. Chem. Soc.* **2005**, *127*, 4809−4830.
(52) Negishi, E.-I.; Takahashi, T. *Acc. Chem. Res.* **1994**, *27*, 124−130.
(53) Boulho, C.; Oulie, P.; Vendier, L.; Etienne, M.; Pimienta, V.; Locati, A.; Bessac, F.; Maseras, F.; Pantazis, D. A.; McGrady, J. E. *J. Am. Chem. Soc.* **2010**, *132*, 14239−14250.
(54) Boulho, C.; Vendier, L.; Etienne, M.; Locati, A.; Maseras, F.; McGrady, J. E. *Organometallics* **2011**, *30*, 3999−4007.
(55) Boulho, C.; Keys, T.; Coppel, Y.; Vendier, L.; Etienne, M.; Locati, A.; Bessac, F.; Maseras, F.; Pantazis, D. A.; McGrady, J. E. *Organometallics* **2009**, *28*, 940−943.
(56) Etienne, M.; Weller, A. S. *Chem. Soc. Rev.* **2014**, *43*, 242−259.
(57) Buchwald, S. L.; Nielsen, R. B. *Chem. Rev.* **1988**, *88*, 1047−1058.
(58) Yin, J.; Jones, W. M. *Organometallics* **1993**, *12*, 2013−2014.
(59) Brookhart, M.; Green, M.; Wong, L. *Prog. Inorg. Chem.* **1988**, *36*, 1−124.
(60) Brookhart, M.; Green, M. L. H.; Parkin, G. *Proc. Natl. Acad. Sci. U.S.A.* **2007**, *104*, 6908−6914.
(61) Erker, G.; Petrenz, R.; Krueger, C.; Lutz, F.; Weiss, A.; Werner, S. *Organometallics* **1992**, *11*, 1646−1655.
(62) Fisher, R. A.; Buchwald, S. L. *Organometallics* **1990**, *9*, 871−873.
(63) Pantazis, D. A.; McGrady, J. E.; Maseras, F.; Etienne, M. *J. Chem. Theory Comput.* **2007**, *3*, 1329−1336.
(64) Pantazis, D. A.; McGrady, J. E.; Besora, M.; Maseras, F.; Etienne, M. *Organometallics* **2008**, *27*, 1128−1134.
(65) Etienne, M.; McGrady, J. E.; Maseras, F. *Coord. Chem. Rev.* **2009**, *253*, 635−646.
(66) Escudie, Y.; Dinoi, C.; Allen, O.; Vendier, L.; Etienne, M. *Angew. Chem., Int. Ed.* **2012**, *51*, 2461−2464.
(67) Negishi, E.; Nguyen, T.; Maye, J.; Choueiri, D.; Suzuki, N.; Takahashi, T. *Chem. Lett.* **1992**, 2367−2370.
(68) Buchwald, S. L.; Lum, R. T.; Fisher, R. A.; Davis, W. M. *J. Am. Chem. Soc.* **1989**, *111*, 9113−9114.
(69) Reed, A. E.; Curtiss, L. A.; Weinhold, F. *Chem. Rev.* **1988**, *88*, 899−926.
(70) Seyferth, D.; Cohen, H. M. *J. Organomet. Chem.* **1963**, *1*, 15−21.
(71) Sheldrick, G. M. *Acta Crystallogr., Sect. A* **2008**, *64*, 112−122.
(72) Farrugia, L. J. *J. Appl. Crystallogr.* **1999**, *32*, 837−838.
(73) Adamo, C.; Barone, V. *J. Chem. Phys.* **1999**, *110*, 6158−6170.
(74) Frisch, M. J.; et al. *Gaussian 03*, Revision E.01; Gaussian, Inc.: Wallingford, CT, 2004.
(75) Schafer, A.; Huber, C.; Ahlrichs, R. *J. Chem. Phys.* **1994**, *100*, 5829−5835.
(76) Schindler, M.; Kutzelnigg, W. *J. Chem. Phys.* **1982**, *76*, 1919−1933.